Proposal to Use Laser-Accelerated Electrons to Probe the Axion-Electron Coupling

Georgios Vacalis[®], ^{1,*} Atsushi Higuchi[®], ² Robert Bingham[®], ^{3,4} and Gianluca Gregori[®] ¹Department of Physics, University of Oxford, Parks Road, Oxford OX1 3PU, United Kingdom ²Department of Mathematics, University of York, Heslington, York YO10 5DD, United Kingdom ³Rutherford Appleton Laboratory, Chilton, Didcot, Oxon OX11 OQX, United Kingdom, ⁴Department of Physics, University of Strathclyde, Glasgow G4 0NG, United Kingdom

(Received 14 May 2025; accepted 20 October 2025; published 6 November 2025)

The axion is a hypothetical particle associated with a possible solution to the strong CP problem and is a leading candidate for dark matter. In this Letter we investigate the emission of axions by accelerated electrons. We find the emission probability and energy within the WKB approximation for an electron accelerated by an electromagnetic field. As an application, we estimate the number of axions produced by electrons accelerated using two counterpropagating high-intensity lasers and discuss how they would be converted to photons to be detected. We find that, under realistic experimental conditions, competitive model-independent bounds on the coupling between the axion and the electron could be achieved in such an experiment.

DOI: 10.1103/vgvg-hcbr

Introduction—The standard model of particle physics is one of the most successful theories of fundamental physics, whose accuracy has been verified by numerous laboratory experiments. It has some shortcomings, however. One of them is that it allows for CP violation in the strong sector. The neutron electric dipole moment, which is a natural consequence of this model, has been constrained by experiments to be unexpectedly negligible. The standard model also fails to accommodate the existence of dark matter. Peccei and Quinn [1,2] proposed solving the strong CP problem by introducing an anomalous U(1) symmetry. Later, Weinberg and Wilczek noted the presence of a pseudo-Goldstone boson, the axion, due to the spontaneous breaking of this U(1) symmetry [3,4]. This hypothetical particle, the axion, is also a possible dark matter candidate [5–7].

In many of the viable models, the axion, which is a massive particle, couples to both the photon and the electron. So far there is no experimental evidence for an axion, and numerous experiments and astrophysical searches have been used to put limits on the axion parameter space. For example, the CAST experiment [8] converts axions, if they exist, into photons using a strong magnetic field. These axions are hypothetically produced in the Sun by Primakoff scattering. However, the upper bound on the axion-photon coupling in astrophysical searches can

Published by the American Physical Society under the terms of the Creative Commons Attribution 4.0 International license. Further distribution of this work must maintain attribution to the author(s) and the published article's title, journal citation, and DOI. Funded by SCOAP³. be model-dependent. For example, in the case of the Sun, collective plasma screening can change the rate of axion production by Primakoff scattering, and hence, the inferred limits suffer from these systematic uncertainties. For this reason, purely terrestrial experiments, where the (hypothetical) production and detection of axions are modelindependent, have an important role. One such experiment is the Optical Search for QED Vacuum Bifringence, Axions and Photon Regeneration (OSQAR) [9], which uses a lightshining-through-walls (LSW) approach to produce and detect axions in the laboratory. Other LSW experiments have been proposed [10,11] for which the production of axions is achieved using high-power laser beams. For a comprehensive review of current axion searches, refer to Ref. [12] and the references therein. The experiments mentioned above only test the coupling between an axion and two photons and therefore can put constraints on the photon-axion coupling but not on the electron-axion coupling. In this Letter, we propose a different mechanism for axion production in the laboratory which makes use of the electron-axion coupling. Accelerated electrons can emit axions in a way similar to the Larmor radiation of photons. This production mechanism allows us to constrain the electron-axion coupling, g_{ae} , in a model-independent manner. Although laboratory-based constraints on g_{ae} are currently available from nuclear reactor experiments [13], the method that we propose here has the advantage of being scalable. Its scalability allows us to lower the upper bound on g_{ae} with the progress of laser technology, which is expected to continue in the next decade with numerous new laser facilities already being proposed [14].

Throughout this Letter, metric signature (+, -, -, -) and units where $c = \epsilon_0 = k_B = 1$ are used unless stated

^{*}Contact author: georgios.vacalis@chch.ox.ac.uk

otherwise. Initially, Planck's constant \hbar is not set to 1 because we use a semiclassical expansion in powers of \hbar .

Axion production—We study the emission of axions by an electron described by a spinor field ψ which is accelerated through a classical electromagnetic potential A_{μ} . We use the semiclassical solution, i.e., the solution in the WKB approximation, to the Dirac equation in an external electromagnetic field. Here, we present the main results and leave the details of the calculations to Supplemental Material [15] which includes Refs. [16–21]. We note that photon emission using a semiclassical approximation is well known and has been studied in the context of the Baĭer-Katkov method [22–25].

The free Lagrangian is given by

$$\mathcal{L}_{\text{free}} = i\hbar\bar{\psi}\gamma^{\mu}D_{\mu}\psi - m\bar{\psi}\psi + \frac{1}{2}\partial_{\mu}\phi\partial^{\mu}\phi - \frac{m_{a}^{2}}{2\hbar^{2}}\phi^{2}, \quad (1)$$

where ϕ is the axion field and m_a is its mass. The electron mass is denoted by m and the covariant derivative is $D_{\mu} = \partial_{\mu} - ieA_{\mu}/\hbar$, where -e is the electron charge. The presence of the potential modifies the Dirac equation as follows:

$$i\gamma^{\mu}(\hbar\partial_{\mu} - ieA_{\mu})\chi - m\chi = 0. \tag{2}$$

We let $\chi = \Psi e^{-iS/\hbar}$ and find the scalar function S and spinor Ψ to the zeroth order in \hbar . By applying $[i\gamma^{\mu}(\hbar\partial_{\mu} - ieA_{\mu}) + m]$ on the left in Eq. (2) we find that S must satisfy

$$(\partial^{\mu} S + eA^{\mu})(\partial_{\mu} S + eA_{\mu}) - m^{2} = 0.$$
 (3)

We assume that $A_{\mu}=0$ on the hypersurface $t=t_i$ in the past. Then, we consider the world lines with a uniform velocity emanating from this hypersurface toward the future. We define τ as the proper time along these world lines measured from the $t=t_i$ hypersurface, and we assume that these world lines do not cross each other. We let these world lines obey the classical equations of motion for a charged particle with charge -e,

$$\frac{d^2x^{\mu}}{d\tau^2} = -\frac{e}{m}F^{\mu\nu}\frac{dx_{\nu}}{d\tau},\tag{4}$$

where $F_{\mu\nu}=\partial_{\mu}A_{\nu}-\partial_{\nu}A_{\mu}$. Then, the solution to Eq. (3) exists and is given by

$$\partial_{\mu}S = mv_{\mu} - eA_{\mu}, \qquad v^{\mu} = \frac{dx^{\mu}}{d\tau}. \tag{5}$$

In particular, the vector field $mv_{\mu} - eA_{\mu}$ remains hypersurface orthogonal as a consequence of Eq. (4). Then, Eq. (2) at the zeroth order in \hbar is solved, in the representation of the γ matrices such that γ^0 is diagonal [26], by

$$\Psi = \sqrt{p_0 + m} \binom{s}{\frac{\sigma \cdot \mathbf{p}}{p_0 + m} s} \exp\left(-\frac{1}{2} \int_0^{\tau} \partial_{\mu} v^{\mu}(\tau') d\tau'\right), \quad (6)$$

where $p^{\mu} = mv^{\mu}$. A condition for the first-order correction to Ψ to exist leads to the Thomas-BMT equation [17,18] for the two-dimensional spin state s:

$$\frac{ds}{d\tau} = -i\mathbf{F} \cdot \boldsymbol{\sigma}s, \qquad \mathbf{F} = \frac{e}{2m} \left(\mathbf{B} - \frac{\mathbf{p} \times \mathbf{E}}{p_0 + m} \right), \quad (7)$$

where \mathbf{E} and \mathbf{B} are the electric and magnetic field, respectively. We have verified that Eq. (7) is Lorentz invariant as expected.

Now, we expand the electron field using a basis consisting of wave-packet solutions as

$$\psi(x) = \sum_{\mathbf{p},\alpha} \left[u_{(\mathbf{p},\alpha)}(x) b_{(\mathbf{p},\alpha)} + v_{(\mathbf{p},\alpha)}(x) d_{(\mathbf{p},\alpha)}^{\dagger} \right]. \tag{8}$$

Here, the modes $u_{(\mathbf{p},a)}, v_{(\mathbf{p},a)}$ are wave packets which have approximately definite world lines and four-momentum \mathbf{p} of a classical particle and polarization state a, with positive and negative energy, respectively, and satisfy usual orthogonality conditions (see Supplemental Material). The wave-packet modes with different (discrete) momenta are orthogonal to one another. Then, the annihilation and creation operators satisfy the following anticommutation relations:

$$\left\{b_{(\mathbf{p},\alpha)},b_{(\mathbf{p},\beta)}^{\dagger}\right\} = \left\{d_{(\mathbf{p},\alpha)},d_{(\mathbf{p},\beta)}^{\dagger}\right\} = \delta_{\alpha\beta}. \tag{9}$$

The operators with different momenta anticommute.

We approximate the modes $u_{(\mathbf{p},\alpha)}$ by a superposition of the WKB solutions that we discussed earlier. Then, they take approximately the following form:

$$u_{(\mathbf{p},\alpha)}(x) = \sqrt{\frac{p_0 + m}{2p_0}} \binom{s_\alpha}{\frac{\mathbf{p} \cdot \boldsymbol{\sigma}}{p_0 + m}} s_\alpha G(x), \qquad (10)$$

where s_{α} satisfies Eq. (7) and G(x) is peaked around a classical world line with the tangent vector $v^{\mu} = p^{\mu}/m$. The factor $e^{-iS/\hbar}$ and the exponential factor in Eq. (6) are absorbed into this function, which is normalized as

$$\int d^3\mathbf{x} |G(t,\mathbf{x})|^2 = 1. \tag{11}$$

The function G(x) is smooth, but $|G(x)|^2$ can be approximated by $\delta^{(3)}[\mathbf{x} - \mathbf{x}(t)]$ where $[t, \mathbf{x}(t)]$ is the classical world line of the electron.

The free axion field satisfies the Klein-Gordon equation $(\Box + m_a^2/\hbar^2)\phi = 0$ and can be expanded as

$$\hat{\phi}(x) = \int \frac{d^3 \mathbf{k}}{2k_0 (2\pi)^3} [a_{\mathbf{k}} e^{-ik \cdot x} + a_{\mathbf{k}}^{\dagger} e^{ik \cdot x}], \qquad (12)$$

where $k_0 = \sqrt{k^2 + (m_a/\hbar)^2}$ and the operators satisfy

$$\left[a_{\mathbf{k}}, a_{\mathbf{k}'}^{\dagger}\right] = (2\pi)^3 2\hbar k_0 \delta^{(3)}(\mathbf{k} - \mathbf{k}'). \tag{13}$$

We approximate the axion field by a massless field, letting $m_a=0$, for simplicity. Thus, the results obtained here are valid as long as the axion mass is much smaller than the typical axion momentum. As will be shown, we can impose bounds on the axion parameter space for $m_a \lesssim 10$ keV, although a massless limit was assumed initially. Notice that the wave number of the axion is regarded as classical so that its momentum is of order \hbar in our WKB approximation. (This is similar to the case for photons [20].) The interaction Lagrangian between the axion and the electron field is [27]

$$\mathcal{L}_{\rm int} = -\frac{\hbar g_{ae}}{2m} \partial_{\mu} \phi \bar{\psi} \gamma_5 \gamma^{\mu} \psi. \tag{14}$$

To the leading order in g_{ae} , the interaction Hamiltonian is $\mathcal{H}_{\rm int} = -\mathcal{L}_{\rm int}$ with normal ordering. We assume that the initial electron state $b_{(\mathbf{p},a)}^{\dagger}|0\rangle$, where $|0\rangle$ is the vacuum state, is such that the final state (after the emission of an axion with typical momentum \mathbf{k}) is approximately $a_{\mathbf{k}}^{\dagger}b_{(\mathbf{p},\beta)}^{\dagger}|0\rangle$. Given the large energy difference between the electron and the axion, it seems reasonable to take (approximately) the same initial and final wave-packet states for the electron wave functions. A similar approach leads to the model of photon emission from the classical electron starting from QED (see Ref. [16]). The only possible difference between the initial and final state is the spin state. Thus, the electron spin is either flipped or not flipped after emission, but the spatial wave function remains the same in our approximation.

To the first order in perturbation theory, the total one-axion-emission final state is given by

$$|f\rangle = -\frac{i}{\hbar} \int d^4x \mathcal{H}_{\rm int}(x) b^{\dagger}_{(\mathbf{p},\alpha)} |0\rangle,$$
 (15)

and the emission probability is $P_{\rm em}=\langle f|f\rangle$. Inserting Eqs. (8) and (12) into Eq. (15) and using the operator relations (9) and (13), we find

$$P_{\text{em}}^{(\beta,\alpha)} = \hbar \int \frac{d^3 \mathbf{k}}{(2\pi)^3 2k_0} |\mathcal{A}_{(\mathbf{p},\mathbf{k},\beta,\alpha)}|^2.$$
 (16)

The interaction amplitude is

$$\mathcal{A}_{(\mathbf{p},\mathbf{k},\beta,\alpha)} = \frac{g_{ae}}{2m} \int d\tau \frac{e^{ik\cdot x(\tau)}}{(k\cdot v)^2} s_{\beta}^{\dagger}(\tau) \mathbf{Q}(\tau) \cdot \boldsymbol{\sigma} s_{\alpha}(\tau), \quad (17)$$

where

$$\mathbf{Q} = \mathbf{V} - (k \cdot a)\mathbf{k} - [V_0 - (k \cdot a)k_0] \frac{\mathbf{p}}{p_0 + m},$$

$$V^{\mu} = \frac{e}{m}(k \cdot v)F^{\mu\nu}k_{\nu}.$$
(18)

Here, $a^{\mu} = dv^{\mu}/d\tau$ is the proper acceleration of the electron. The spin states s_{α} and s_{β} satisfy Eq. (7). We verify Eq. (16) to the lowest order in eA_{μ} by using a Feynman-diagram calculation in Supplemental Material.

In the next section, we study laser-accelerated electrons, which follow two-dimensional trajectories. In this case, we choose an electric field in the x-z plane and a magnetic field parallel to the y axis. It is convenient to choose the initial spin polarization along the y direction. Then,

$$P_{\text{em}}^{\text{nf}} = \frac{\hbar g_{ae}^2}{4m^2} \int \frac{d^3 \mathbf{k}}{(2\pi)^3 2k_0} k_y^2 \left| \int d\tau e^{ik \cdot x} \frac{k \cdot a}{(k \cdot v)^2} \right|^2,$$

$$P_{\text{em}}^{\text{f}} = \frac{\hbar g_{ae}^2}{4m^2} \int \frac{d^3 \mathbf{k}}{(2\pi)^3 2k_0} \left| \int d\tau e^{ik \cdot x \mp if(\tau)} [Q_z \pm iQ_x] \right|^2, \quad (19)$$

where $df(\tau)/d\tau = F_y$, with F_y defined in Eq. (7), and $Q_z \pm iQ_x$ is found from Eq. (18). The first expression is the emission probability when the electron does not flip its spin $(\alpha = \beta)$, whereas the second corresponds to the spin-flip case. In the second equation in (19), the upper and lower signs are for the spin states s_+ and s_- , respectively, where $\sigma_y s_\pm = \pm s_\pm$.

It is possible to find a simpler expression for the spin-averaged axion energy emitted for a three-dimensional motion using the technique employed in deriving the Larmor formula in the WKB approximation [16,19,20]. With the definition $n^{\mu} = k^{\mu}/k_0$, we find the spin-averaged axion energy emitted as

$$\begin{split} \langle E \rangle &= \frac{\hbar^2 g_{ae}^2}{16\pi m^2} \int \frac{d\Omega}{4\pi} \int \frac{d\tau}{(n \cdot v)^7} \\ &\times \left[-\frac{9(n \cdot a)^2}{(n \cdot v)^2} U_\mu U^\mu + \frac{3n \cdot a}{n \cdot v} \frac{d}{d\tau} (U_\mu U^\mu) - H_\mu H^\mu \right], \end{split} \tag{20}$$

where

$$U^{\mu} = (n \cdot a)n^{\mu} - \frac{e}{m}(n \cdot v)F^{\mu\nu}n_{\nu},$$

$$H^{\mu} = \frac{dU^{\mu}}{d\tau} + \frac{e}{m}F^{\mu\nu}U_{\nu}.$$
(21)

Experimental proposal—The proposed setup consists of an emission region where the axions are produced by laser-accelerated electrons and a conversion region where they are regenerated into photons (see Fig. 1).

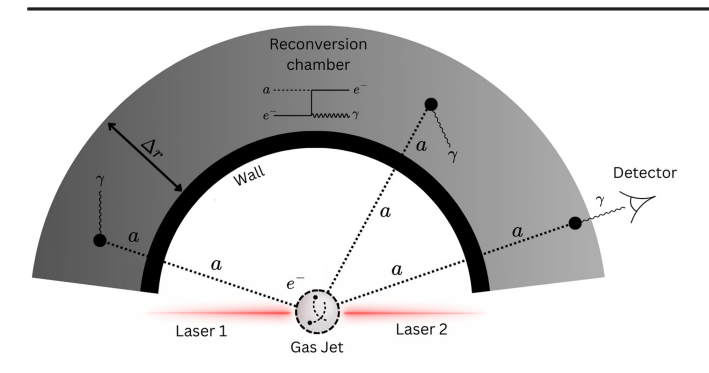


FIG. 1. Diagram of the experimental proposal. We assume that there are enough detectors to cover a large solid angle.

Throughout this section, we put $\hbar=1$ and assume that the parameters m_a , g_{ae} , and $g_{a\gamma}$ are independent. For the results of the previous section to be applicable, $m_a \ll k_a$, where k_a is the typical axion momentum, which depends on the laser parameters. We have $k_a \sim 10^2$ keV for the laser parameters that we will consider. Therefore, the bounds on g_{ae} obtained in this section will be valid for $m_a \lesssim 10$ keV. The axions are converted to photons through processes $a+e^- \rightarrow \gamma + e^-$ and $a+N_T \rightarrow \gamma + N_T$ that involve the couplings g_{ae} and $g_{a\gamma}$, respectively $(N_T$ here is an atomic target) [28,29]. Only the former process is considered as it allows us to impose upper bounds on g_{ae} in the absence of photon detection. In what follows, we use the model-independent bound $g_{a\gamma} \lesssim 10^{-4}$ GeV⁻¹ [13].

A hydrogen gas jet is used as a source of electrons. These are accelerated by two counterpropagating lasers of pulse duration τ_p , forming a standing laser field as described in [30]. The beams are linearly polarized along the z direction and propagating along the x direction. They are described as plane waves with angular frequency ω_0 . The electric and magnetic fields are therefore

$$E_z = E_0[\cos \omega_0(t - x) + \cos \omega_0(t + x)],$$

$$B_y = -E_0[\cos \omega_0(t - x) - \cos \omega_0(t + x)].$$
 (22)

The classical equation of motion of the electron is

$$\frac{dp_x}{dt} = e\beta_z B_y, \qquad \frac{dp_z}{dt} = -e(E_z + \beta_x B_y), \quad (23)$$

where $(\beta_x, \beta_y, \beta_z)$ is the velocity divided by the speed of light. Electrons placed at the nodes $\omega_0 x = 2\pi n, n \in \mathbb{Z}$ do not feel the effects of the magnetic field and have unstable oscillatory trajectories, which implies that it is difficult to realize them experimentally. The trajectories of the offnode electrons, which constitute the vast majority of the electrons accelerated by the laser beams, need to be found by solving Eq. (23) numerically. In principle, it would be possible to use Eq. (19) with these trajectories and estimate the number of axions emitted numerically. However, such

computations would be quite challenging. Instead, we proceed as follows. We first find the energy emitted in the presence of the magnetic, as well as electric, fields by Eq. (20). We then estimate the number of emitted axions by dividing the total energy by the typical axion energy, which we assume to be much larger than m_a . This is justified if the spectrum is peaked around the typical energy. For an electron in a constant magnetic field we find that the spectrum is peaked and the typical energy of individual axions is around $4a_0^3\omega_0$ (see Supplemental Material), where $a_0 = eE_0/m\omega_0$ is the laser strength parameter. Although for laser beams the magnetic field is not constant, we assume the axion spectra to be similar. We note that, since for relativistic electrons the axions are predominantly emitted along the trajectory, the axion emission is concentrated in the x-z plane.

We find that the WKB treatment of the previous section is valid if $a_0^2 \omega_0/m \ll 1$ or $(a_0/700)^2 \ll 1$ for $\omega_0 \approx 1$ eV (see Supplemental Material).

The energy emitted by an electron in one cycle of duration $2\pi/\omega_0$ can be written using Eq. (20) as $\langle E \rangle_{(2\mathrm{d})} = g_{ae}^2 \omega_0^3 m^{-2} \mathcal{N}(a_0)$, where $\mathcal{N}(a_0)$ is a number found numerically. The total number of electron "oscillations" is given by $\rho_e V \nu \tau_p n_s/2$, where ρ_e is the electron density, n_s is the number of shots, V is the volume occupied by one beam, and $\nu = \omega_0/2\pi$ is the frequency. We note that $V = A\tau_p$, where A is the beam cross section. Then, the total number of axions produced is

$$N_a^{\text{tot}} = \frac{g_{ae}^2 \rho_e V \tau_p \omega_0^3 n_s \mathcal{N}(a_0)}{16\pi a_0^3 m^2},$$
 (24)

which was obtained by dividing the total energy by the typical axion energy $k_a = 4a_0^3\omega_0$.

As shown in Fig. 1 (and as in many LSW experiments), axions produced by accelerated electrons pass through a wall which prevents background photons, e.g., those produced by Larmor radiation, from entering the detector. We note that the effect of Larmor radiation on the trajectories can be neglected if $(a_0/250)^2 \ll 1$. The reconversion occurs because the axions then interact with the electrons in the material that surrounds the wall. The Compton-like process $a+e^- \rightarrow \gamma + e^-$ has a total cross section [31]

$$\sigma^{c} = \frac{Z\alpha g_{ae}^{2}}{4m^{2}} f\left(\frac{k_{a}}{m}\right), \quad f(x) = \frac{1}{x} \ln\left(1 + 2x\right) - \frac{2(1+3x)}{(1+2x)^{2}},$$
(25)

in the limit $m_a \to 0$, where α and Z are the fine structure constant and the atomic number, respectively. As before, we let $k_a = 4a_0^3\omega_0$. The photon energy is $\sim k_a$ for $m \gg k_a \gg m_a$. The total number of produced photons is

$$N_{\gamma} = \sigma^{c} \rho_{m} \Delta r N_{a}^{\text{tot}}, \tag{26}$$

where ρ_m is the atom density of the material used for the reconversion and Δr is its length. The latter is at most on the order of the photon attenuation length. Not all produced photons will enter the detector as the ones emitted backward will be absorbed by the wall. However, this effect will only result in a $\mathcal{O}(1)$ correction factor in Eq. (26). Substitution of Eq. (24) into Eq. (26) gives

$$N_{\gamma} = \frac{Z\alpha^2 g_{ae}^4}{8a_0^5} \mathcal{N}(a_0) f\left(\frac{4a_0^3 \omega_0}{m}\right) n_s \frac{\rho_m \rho_e \tau_p \Delta r \omega_0 E_{\text{las}}}{m^6}, \quad (27)$$

where $E_{\rm las}=A\tau_p m^2\omega_0^2 a_0^2/(8\pi\alpha)$ is the energy of the laser pulse.

Let us estimate the bound on g_{ae} achievable for a laser with $E_{\rm las}=1$ kJ, wavelength $\lambda\approx 1$ µm, $\tau_p=10^{-12}$ s, beam diameter $\sim 10\lambda$, and a repetition rate of 10 Hz. Such a laser is not currently available, but it is within the current technological capabilities. For this choice $a_0 \approx 30$, and $E_{\gamma} \approx k_a \approx 133$ keV. We find numerically that $\mathcal{N}(30) \approx 10^{13}$. We also assume that the source of electrons is a hydrogen gas for which $\rho_e = 10^{20}$ cm⁻³. For the given density and intensities, plasma effects can be neglected. For reconversion, we use aluminum. The attenuation length for these photon energies is $\Delta r \sim 1$ cm. If $N_{\gamma} \lesssim 1$ after one week of measurement, we find that $g_{ae} \lesssim 4.1 \times 10^{-5}$. This result is valid for $m_a \ll k_a (\sim 10^2 \text{ keV})$. Next-generation lasers could reach $E_{\rm las} = 10^2 \text{ kJ}$, $\tau_p = 10^{-10} \text{ s}$ with a repetition rate of 1 MHz. Given the rapid development of diode laser technology, it is not inconceivable that such a laser would become available in the future. Assuming that the remaining parameters stay the same, if $N_{\gamma} \lesssim 1$ after one year of measurement, we find $g_{ae} \lesssim 8.5 \times 10^{-8}$. The axions can also decay to photons with a decay rate $\Gamma(a \to \gamma \gamma) = g_{\alpha \gamma}^2 m_a^3 / 64\pi$. The survival probability of the axion reaching the reconversion chamber at distance ℓ is $P_{\rm sur} = \exp[-\ell m_a \Gamma/k_a]$ [13]. However, for $\ell \sim 1$ m, $m_a \lesssim$ 10 keV and $g_{a\gamma} \lesssim 10^{-4} \text{ GeV}^{-1}$ [13], $P_{\text{sur}} \approx 1$.

Axion searches have been conducted in the range of masses $m_a \lesssim 10$ keV. The experiments XENON1T [32] and XENONnT [33] were used to impose stringent bounds on g_{ae} for solar axions. Constraints on g_{ae} for laboratory-produced axions were found using anomalous magnetic moment and electric dipole moment [34] or nuclear reactors for neutrino experiments [13]. These bounds are shown in Fig. 2. In the same figure, we also report the projected bounds from the proposed laser experiment. Using current laser technology and just a week of data gathering, we expect to reach exclusion bounds comparable to other laboratory searches. On the other hand, with a future laser system we could expect to achieve bounds up to the prediction of DFSZ axions [35–37]. The DFSZ axion model followed that of Weinberg and Wilczek, as well as

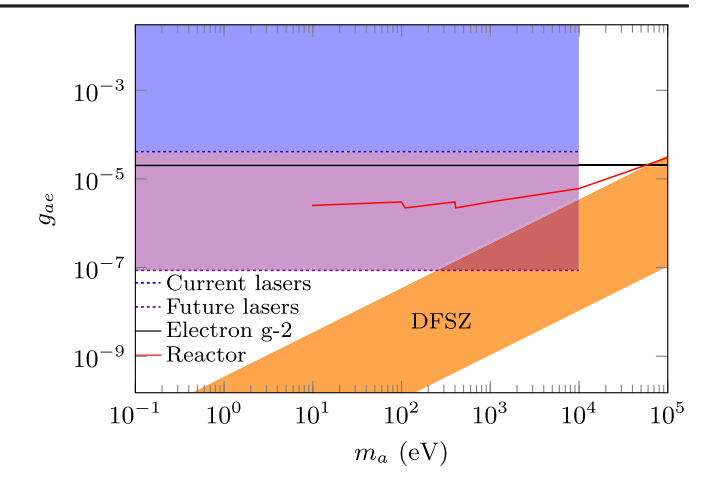


FIG. 2. Bounds of laboratory-based experiments. The red and black curves correspond to the bounds found in [13] and [34], respectively. The orange band is the DFSZ prediction [35–37]. For the next-generation laser, we assumed one year of measurement instead of one week.

KSVZ [38,39], and predicts a coupling of the axion to electrons and light quarks, with the coupling constant being proportional to the axion mass.

Conclusion—In this Letter, we used the WKB approximation to calculate the number of axions and the energy emitted from an electron accelerated in an electromagnetic field. We then applied the WKB approximation to the case of a two-dimensional electron trajectory, where the electron was accelerated by laser beams. Applying the results to an experimental proposal allowed us to find bounds on the coupling g_{ae} . The bounds found are valid for axion masses $m_a \lesssim 10$ keV. Since the results derived in the first section are general, they can be used for other experimental proposals (e.g., replacing the linearly beams by circularly polarized ones). We compared the bounds obtained here with those obtained in other laboratory experiments (e.g., axion production achieved using a nuclear reactor) and found that they are comparable. Whereas it is unlikely that the performance of nuclear reactors will be largely improved in the near future, lasers are subject to important performance enhancements and therefore could allow further exploration of the parameter space of the QCD axion.

Acknowledgments—G. V. acknowledges helpful discussions with Dr. Konstantin A. Beyer. This work was supported in part by EPSRC Grants No. EP/X01133X/1 and No. EP/X010791/1. G. G. is also a member of the Quantum Sensing for the Hidden Sector (QSHS) Collaboration, supported by STFC Grant No. ST/T006277/1.

Data availability—The data that support the findings of this article are openly available [40].

- R. D. Peccei and H. R. Quinn, CP conservation in the presence of pseudoparticles, Phys. Rev. Lett. 38, 1440 (1977).
- [2] R. D. Peccei and H. R. Quinn, Constraints imposed by CP conservation in the presence of pseudoparticles, Phys. Rev. D 16, 1791 (1977).
- [3] S. Weinberg, A new light boson?, Phys. Rev. Lett. **40**, 223 (1978).
- [4] F. Wilczek, Problem of strong *P* and *T* invariance in the presence of instantons, Phys. Rev. Lett. **40**, 279 (1978).
- [5] J. Preskill, M. B. Wise, and F. Wilczek, Cosmology of the invisible axion, Phys. Lett. 120B, 127 (1983).
- [6] L. F. Abbott and P. Sikivie, A cosmological bound on the invisible axion, Phys. Lett. 120B, 133 (1983).
- [7] M. Dine and W. Fischler, The not so harmless axion, Phys. Lett. **120B**, 137 (1983).
- [8] CAST Collaboration, New CAST limit on the axion-photon interaction, Nat. Phys. **13**, 584 (2017).
- [9] R. Ballou et al. (OSQAR Collaboration), New exclusion limits on scalar and pseudoscalar axionlike particles from light shining through a wall, Phys. Rev. D 92, 092002 (2015).
- [10] K. A. Beyer, G. Marocco, R. Bingham, and G. Gregori, Axion detection through resonant photon-photon collisions, Phys. Rev. D 101, 095018 (2020).
- [11] K. A. Beyer, G. Marocco, R. Bingham, and G. Gregori, Light-shining-through-wall axion detection experiments with a stimulating laser, Phys. Rev. D 105, 035031 (2022).
- [12] P. Sikivie, Invisible axion search methods, Rev. Mod. Phys. 93, 015004 (2021).
- [13] J. B. Dent, B. Dutta, D. Kim, S. Liao, R. Mahapatra, K. Sinha, and A. Thompson, New directions for axion searches via scattering at reactor neutrino experiments, Phys. Rev. Lett. **124**, 211804 (2020).
- [14] A. D. Piazza, L. Willingale, and J. D. Zuegel, Multi-Petawatt physics prioritization (MP3) workshop report, arXiv:2211.13187.
- [15] See Supplemental Material at http://link.aps.org/supplemental/10.1103/vgvg-hcbr for the derivations of some of the results of this Letter.
- [16] G. D. R. Martin, Classical and quantum radiation reaction, Ph.D. thesis, York University, England, Dept. Math., 2007.
- [17] L. H. Thomas, The motion of the spinning electron, Nature (London) 117, 514 (1926).
- [18] V. Bargmann, L. Michel, and V. L. Telegdi, Precession of the polarization of particles moving in a homogeneous electromagnetic field, Phys. Rev. Lett. 2, 435 (1959).
- [19] A. Higuchi and P. J. Walker, Quantum corrections to the Larmor radiation formula in scalar electrodynamics, Phys. Rev. D 80, 105019 (2009).
- [20] A. Higuchi and G. D. R. Martin, Radiation reaction on charged particles in three-dimensional motion in classical and quantum electrodynamics, Phys. Rev. D 73, 025019 (2006).

- [21] I. S. Gradshteyn and I. M. Ryzhik, Table of Integrals, Series, and Products—Eighth edition (Academic Press, New York, 2014).
- [22] V. Baĭer and V. Katkov, Quantum effects in magnetic bremsstrahlung, Phys. Lett. 25A, 492 (1967).
- [23] V. Baĭer and V. Katkov, Processes involved in the motion of high energy particles in a magnetic field, JETP 26, 854 (1968).
- [24] V. Baĭer and V. Katkov, Quasiclassical theory of bremsstrahlung by relativistic particles, JETP 28, 807 (1969).
- [25] V. N. Baĭer, Radiative polarization of electrons in storage rings, Sov. Phys. Usp. 14, 695 (1972).
- [26] J. D. Bjorken and S. D. Drell, *Relativistic Quantum Me-chanics*, International Series In Pure and Applied Physics (McGraw-Hill, New York, 1965).
- [27] G. G. Raffelt, Stars as Laboratories for Fundamental Physics: The Astrophysics of Neutrinos, Axions, and Other Weakly Interacting Particles (The University of Chicago Press, Chicago, 1996).
- [28] Y. S. Tsai, Axion bremsstrahlung by an electron beam, Phys. Rev. D 34, 1326 (1986).
- [29] D. Aloni, C. Fanelli, Y. Soreq, and M. Williams, Photoproduction of axionlike particles, Phys. Rev. Lett. 123, 071801 (2019).
- [30] P. Chen and T. Tajima, Testing unruh radiation with ultraintense lasers, Phys. Rev. Lett. 83, 256 (1999).
- [31] F. T. Avignone, C. Baktash, W. C. Barker, F. P. Calaprice, R. W. Dunford, W. C. Haxton, D. Kahana, R. T. Kouzes, H. S. Miley, and D. M. Moltz, Search for Axions From the 1115-kev Transition of ⁶⁵Cu, Phys. Rev. D 37, 618 (1988).
- [32] K. Van Tilburg, Stellar basins of gravitationally bound particles, Phys. Rev. D **104**, 023019 (2021).
- [33] E. Aprile *et al.* (XENON Collaboration), Search for new physics in electronic recoil data from xenonnt, Phys. Rev. Lett. **129**, 161805 (2022).
- [34] H. Yan, G. A. Sun, S. M. Peng, H. Guo, B. Q. Liu, M. Peng, and H. Zheng, Constraining exotic spin dependent interactions of muons and electrons, Eur. Phys. J. C 79, 971 (2019).
- [35] A. R. Zhitnitsky, On possible suppression of the axion hadron interactions (in Russian), Sov. J. Nucl. Phys. **31**, 260 (1980).
- [36] M. Dine, W. Fischler, and M. Srednicki, A simple solution to the strong CP problem with a harmless axion, Phys. Lett. 104B, 199 (1981).
- [37] G. G. Raffelt, Astrophysical axion bounds diminished by screening effects, Phys. Rev. D 33, 897 (1986).
- [38] J. E. Kim, Weak-interaction singlet and strong CP invariance, Phys. Rev. Lett. 43, 103 (1979).
- [39] M. A. Shifman, A. I. Vainshtein, and V. I. Zakharov, Can confinement ensure natural CP invariance of strong interactions?, Nucl. Phys. B166, 493 (1980).
- [40] 10.5281/zenodo.17406226 (2025).

End Matter

Appendix: Comparison between on- and off-node electrons—We show here the effect of the magnetic field on axion production. On-node electrons have an oscillatory trajectory with

$$\gamma \beta_z = -2a_0 \sin \omega_0 t, \qquad \gamma = \sqrt{1 + 4a_0^2 \sin^2 \omega_0 t}. \tag{A1}$$

The energy emitted in one cycle is given by

$$\langle E \rangle_{\text{(1d)}} = \frac{g_{ae}^2 \omega_0^3}{6m^2} (7a_0^4 + a_0^2).$$
 (A2)

The typical axion energy for on-node electrons is $4a_0^2\omega_0$, and the spectrum is peaked around this value. The particle numbers emitted in one cycle by on- and off-node electrons are shown in Fig. 3. The number of emitted axions is much larger for the off-node case, which shows the importance of the magnetic field on particle production.

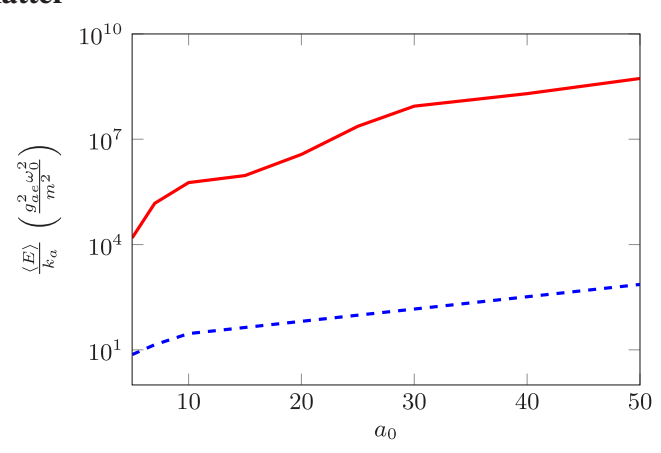


FIG. 3. Number of axions produced in one cycle (estimated by dividing the total energy by the typical axion energy) by one onnode electron (blue dashed line) and by one off-node electron (red solid line) with initial condition $\omega_0 x(0) = \pi/3$. The number was averaged over ten cycles.